

Isolation of a  $^{177}\text{Hf}$  Complex Formed by  $\beta$ -Decay of a  $^{177}\text{Lu}$ -Labeled Radiotherapeutic Compound and NMR Structural Elucidation of the Ligand and its Lu and Hf ComplexesAldo Cagnolini,<sup>†</sup> Nicola D'Amelio,<sup>‡</sup> Edmund Metcalfe,<sup>†</sup> Hanh D. Nguyen,<sup>†</sup> Silvio Aime,<sup>§</sup> Rolf E. Swenson,<sup>†</sup> and Karen E. Linder<sup>\*†</sup>*Ernst Felder Laboratories, Bracco Research USA Inc., 305 College Road East, Princeton, New Jersey 08540, Bracco Imaging SpA-CRB Trieste, AREA Science Park, Building Q, SS 14, Km 163.5, 34012 Basovizza (Trieste), Italy, and Dipartimento di Chimica IFM and Centro di Imaging Molecolare, Università di Torino, Via P. Giuria 7, 10125 Torino, Italy*

Received December 4, 2008

$^{177}\text{Lu}$ -AMBA (AMBA = DO3A-CH<sub>2</sub>CO-G-[4-aminobenzoyl]-QWAVGHLM-NH<sub>2</sub>) is being developed for the radiotherapeutic treatment of tumors that express the gastrin-releasing peptide receptor (GRP-R). In this study we investigated the fate of the  $^{177}\text{hafnium}$  ( $^{177}\text{Hf}$ ) that forms upon the decay of  $^{177}\text{Lu}$  while the latter is complexed with AMBA. When decayed solutions of  $^{177}\text{Lu}$ -AMBA were analyzed, it was found that  $^{177}\text{Hf}$  is retained in the DO3A monoamide chelator, forming a pair of interconverting isomers. We report the synthesis and full characterization of  $^{177}\text{Lu}$ -AMBA and the studies performed to demonstrate its correspondence to radioactive  $^{177}\text{Lu}$ -AMBA. We also report the synthesis and characterization of Hf-AMBA and, by NMR studies, show structural analogies between Hf-AMBA, its parent compound Lu-AMBA, and the unmetallated AMBA ligand. In the NMR spectra of both the metallated and unmetallated AMBA ligand, a stacking interaction between the amino benzoyl residue in the linker and a tryptophan in the truncated bombesin [BBN(7-14)-NH<sub>2</sub>] peptide targeting group was found.

## Introduction

Many peptide-based target-specific therapeutic and imaging radiopharmaceuticals that use derivatives of the macrocyclic chelator DO3A—monoamide have been reported.<sup>1–4</sup> This chelator is frequently used to chelate the radiometal in complexes used for radiotherapeutic applications due to the

high stability of the resulting radiometal complex. An example of this class of compounds is  $^{177}\text{Lu}$ -AMBA (Figure 1), a novel  $^{177}\text{lutetium}$ -labeled peptide that is being developed<sup>4,5</sup> for the radiotherapeutic treatment of tumors that express the gastrin-releasing peptide receptor (AMBA = DO3A-CH<sub>2</sub>CO-G-[4-aminobenzoyl]-QWAVGHLM-NH<sub>2</sub>). The receptor is overexpressed in several types of cancer, including prostate, breast, and small cell lung cancer.<sup>6–8</sup>

$^{177}\text{Lu}$  ( $t_{1/2}$  = 6.7 days) emits both a medium energy  $\beta^-$  useful for radiotherapy and  $\gamma$  emissions of suitable energy for imaging. The short range of the  $^{177}\text{Lu}$   $\beta^-$  emission (2.1 mm maximum) is ideal for the treatment of small metastases.<sup>9</sup> The sole decay product of  $^{177}\text{Lu}$  is nonradioactive

\* To whom correspondence should be addressed. Phone: 609-514-2416. Fax: 609-514-2446. E-mail: karen.linder@bru.bracco.com.

<sup>†</sup> Bracco Research USA Inc.

<sup>‡</sup> Bracco Imaging SpA-CRB Trieste.

<sup>§</sup> Università di Torino.

- (1) Kwekkeboom, D. J.; Bakker, W. H.; Kam, B. L.; Teunissen, J. J.; Kooij, P. P.; de Herder, W. W.; Feelders, R. A.; van Eijck, C. H.; de Jong, M.; Srinivasan, A.; Erion, J. L.; Krenning, E. P. *Eur. J. Nucl. Med. Mol. Imaging* **2003**, *30* (3), 417–422.
- (2) Banerjee, S.; Das, T.; Chakraborty, S.; Samuel, G.; Korde, A.; Srivastava, S.; Venkatesh, M.; Pillai, M. R. A. *Nucl. Med. Biol.* **2004**, *31* (6), 753–759.
- (3) Liu, S.; Pietryka, J.; Ellars, C. E.; Edwards, D. S. *Bioconj. Chem.* **2002**, *13*, 902–913.
- (4) Lantry, L. E.; Cappelletti, E.; Maddalena, M.; Stewart-Fox, J.; Feng, W.; Chen, J.; Thomas, R.; Eaton, S. M.; Bogdan, N. J.; Arunachalam, T.; Reubi, J.-C.; Raju, N.; Lattuada, L.; Linder, K. E.; Swenson, R. E.; Tweedle, M. F.; Nunn, A. D. *J. Nucl. Med.* **2006**, *47* (7), 1144–1152.

(5) Chen, J.; Linder, K. E.; Cagnolini, A.; Metcalfe, E.; Raju, N.; Tweedle, M. F.; Swenson, R. E. *Appl. Radiat. Isot.* **2008**, *66*, 497–505.

(6) Reubi, J. C. *Endocr. Rev.* **2003**, *24*, 389–427.

(7) Scopinaro, F.; De Vincentis, G.; Corazziari, E.; et al. *Cancer Biother. Radiopharm.* **2004**, *19*, 245–252.

(8) Reile, H.; Armatis, P. E.; Schally, A. V. *Prostate* **1994**, *25*, 29–38.

(9) de Jong, M.; Breeman, W. A. P.; Valkema, R.; Bernard, B. F.; Krenning, E. P. *J. Nucl. Med.* **2005**, *46* (1), 13S–17S.

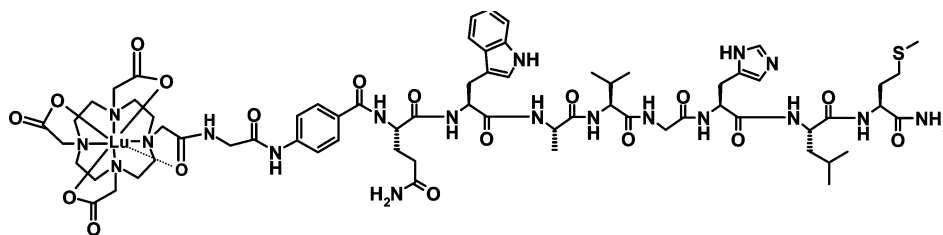


**Figure 1.** Chemical structure of  $^{177}\text{Lu}$ -AMBA.

$^{177}\text{Hf}$ .<sup>10</sup> For these and other reasons, including its cost and availability, ease and safety in handling, and compatibility with DO3A chelation,  $^{177}\text{Lu}$  was selected as the radioisotope for use in  $^{177}\text{Lu}$ -AMBA.

$^{177}\text{Lu}$  is prepared by bombarding a target of enriched  $^{176}\text{Lu}$  with neutrons. Target irradiation typically takes about a week and results in 18–27% of the  $^{176}\text{Lu}$  in the target being converted to  $^{177}\text{Lu}$ ,<sup>11</sup> depending on the neutron flux and irradiation time used. Because some of the  $^{177}\text{Lu}$  that forms during irradiation subsequently decays to nonradioactive  $^{177}\text{Hf}$  during bombardment, the  $^{177}\text{LuCl}_3$  solution that is prepared from the target will always contain some  $^{177}\text{Hf}$ . At the end of bombardment (EOB), the target (for a typical lot of Lu with an initial specific activity of 925 GBq/mg) contains ~6%  $^{177}\text{Hf}$ , ~23%  $^{177}\text{Lu}$ , and ~70%  $^{176}\text{Lu}$ . These numbers will vary somewhat, and the resultant  $^{177}\text{Lu}$  will have a specific activity that ranges from 740 to 1110 GBq/mg at EOB.

It has been established in our laboratories and elsewhere<sup>12</sup> that the hafnium present in the  $^{177}\text{LuCl}_3$  solutions used for the labeling of radiotherapeutic compounds such as  $^{177}\text{Lu}$ -AMBA is not chelated by monosubstituted DOTA derivatives under the aqueous conditions normally used for radiolabeling. However, to our knowledge, no reports have discussed the fate of the  $^{177}\text{hafnium}$  that forms upon the decay of  $^{177}\text{Lu}$  while the latter is complexed to a monosubstituted DO3A amide or any other chelator. Radioactive decay in a labeled molecule generally has catastrophic chemical consequences due to the change in chemical identity of the element that has decayed and to local transmutation effects such as recoil, electronic excitation, and a buildup of charge states.<sup>13</sup> Internal radiolytic effects that lead to molecular bond scission or oxidation are also frequently observed. Thus, the isolation of an intact decay product is unexpected.

Herein, we present data showing that, when  $^{177}\text{Lu}$ -AMBA undergoes  $\beta^-$  decay, greater than 80% of the  $^{177}\text{Hf}$  that forms is retained in the chelator, and the resulting  $^{177}\text{Hf}$ -AMBA products are stable. We have synthesized and fully characterized  $^{\text{nat}}\text{Hf}$ -AMBA ( $^{\text{nat}}\text{Hf}$  = natural Hf) and, by NMR studies, show structural analogies with the parent Lu compound and unmetallated ligand. We also report the synthesis and full

characterization of  $^{\text{nat}}\text{Lu}$ -AMBA and the studies performed to demonstrate its correspondence to radioactive  $^{177}\text{Lu}$ -AMBA.

## Experimental Procedures

The following abbreviations are used: sodium acetate (NaOAc), acetonitrile (ACN), dimethylformamide (DMF), dimethyl sulfoxide (DMSO), trifluoroacetic acid (TFA), ammonium sulfate  $(\text{NH}_4)_2\text{SO}_4$ , trimethylsilyl-2,2,3,3-tetradecateropropionic acid (TSP), lutetium (Lu), hafnium (Hf), L-(+)-selenomethionine (Se-Met), and radiochemical purity (RCP).

$^{177}\text{LuCl}_3$  solutions in 0.1 N HCl, prepared from the irradiation of an enriched  $^{176}\text{Lu}$  target (74.5% enrichment), were obtained from Missouri University Reactor Research (Columbia, MO). AMBA was synthesized as previously reported.<sup>5</sup>  $\text{HfCl}_4$  (98% pure) was purchased from Aldrich.  $\text{LuCl}_3 \cdot 6\text{H}_2\text{O}$  (99.9%) was purchased from Alfa Aesar. Se-Met was obtained from Sabinsa Corp. Bacteriostatic 0.9% sodium chloride injection (U.S.P.) was purchased from Abbott Laboratories. ASCOR L500 ascorbic acid injection [U.S.P.; containing 500 mg/mL Ascorbic acid and 0.025% (w/v)  $\text{Na}_2\text{EDTA}$ ] was obtained from McGuff Pharmaceuticals. All other chemicals were purchased from VWR or Aldrich.

HPLC analysis, purification, and characterization of reaction mixtures and final products was conducted with an Agilent 1100 series quaternary pump gradient system driven by Agilent Chem-Station, model number G1319A, revision A.09.01.

HPLC Method 1. Vydac C-18 Protein and Peptide column (10 × 250 mm) eluted as follows: from 85%  $\text{H}_2\text{O}$  with 0.1% TFA (v/v)/15% ACN (0.1% TFA (v/v)) to 70%/30% in 30 min; from 70%/30% to 60%/40% in 1 min, hold for 5 min. Flow rate = 5 mL/min,  $T = 37^\circ\text{C}$ .

HPLC Method 2. Agilent/Zorbax Bonus RP column (250 mm × 4.6 mm, 5  $\mu\text{m}$  silica) eluted as follows: from 30% 30 mM  $(\text{NH}_4)_2\text{SO}_4$  in  $\text{H}_2\text{O}$  with 0.1% TFA (v/v)/60%  $\text{H}_2\text{O}$ /5% MeOH/5% ACN to 14/60/13/13 in 5 min. Hold at 14/60/13/13 for 35 min, ramp to 0/60/20/20 in 3 min. Hold at 0/60/20/20 for 5 min, return to 30/60/5/5 in 1 min. Flow rate = 1.5 mL/min,  $T = 37^\circ\text{C}$ .

HPLC Method 3. Vydac C-18 Protein and Peptide column (10 × 250 mm) eluted with 12% ACN/12% MeOH/60% 30 mM  $(\text{NH}_4)_2\text{SO}_4$  in  $\text{H}_2\text{O}$  with 0.1% TFA (v/v)/16%  $\text{H}_2\text{O}$ . Flow rate 5 mL/min,  $T = 37^\circ\text{C}$ .

HPLC Method 4. Vydac C-18 Protein and Peptide column (10 × 250 mm) eluted as follows: from 80%  $\text{H}_2\text{O}$  with 0.1% TFA (v/v)/20% ACN with 0.1% TFA (v/v) to 76%/24% in 15 min. Flow rate = 4.5 mL/min,  $T = 37^\circ\text{C}$ .

HPLC Method 5. Agilent/Zorbax Bonus RP column (250 mm × 4.6 mm, 5  $\mu\text{m}$ ) eluted as follows: from 85%  $\text{H}_2\text{O}$ /15% ACN (both 0.1% TFA) to 70/30 in 30 min. Flow rate 1 mL/min,  $T = 30^\circ\text{C}$ .

HPLC Method 6. Agilent/Zorbax Bonus RP column (250 mm × 4.6 mm, 5  $\mu\text{m}$  silica) eluted as follows: from 30% 30 mM  $(\text{NH}_4)_2\text{SO}_4$  in  $\text{H}_2\text{O}$  with 0.1% TFA (v/v)/60%  $\text{H}_2\text{O}$ /5% MeOH/5%

(10) Chu, S. Y. U.; Ekstrom L. P.; Firestone, R. B. *The Lund/LBNL Nuclear Data Search, LBNL Isotopes Project*, version 2.0; LBNL: Berkeley, CA; Lund University: Sweden, 1999.

(11) Ehrhard, G. J.; Ketring, A. R.; Ayers, L. M. *Appl. Radiat. Isot.* **1998**, *49*, 295–297.

(12) Breeman, W. A. P.; De Jong, M.; Visser, T. J.; Erion, J. L.; Krenning, E. P. *Eur. J. Nucl. Med. Mol. Imaging* **2003**, *30* (6), 917–920.

(13) Halpern, A.; Stöcklin, G. *Radiat. Environ. Biophys.* **1977**, *14* (3), 167–183.

ACN to 10/60/15/15 in 5 min. Hold at 10/60/15/15 for 35 min, ramp to 0/60/20/20 in 3 min. Hold at 0/60/20/20 for 5 min, return to 30/60/5/5 in 1 min. Flow rate = 1.5 mL/min,  $T = 37\text{ }^{\circ}\text{C}$ .

Elemental analysis (C, H, N, S, F) and water content determination (by Karl Fisher analysis) were performed by Quantitative Technologies Inc. (Whitehouse, NJ). Amino acid analysis (acid hydrolysis) was performed by AAI Development Services (North Brunswick, NJ).

Mass spectra data were obtained on an Agilent 1100 LC/MSD system equipped with an HP 1110 series UV detector and an HP 1100 single quadrupole mass detector with an electrospray ionization source. Spectra were acquired in positive ion mode in the mass range 500–2000 amu. Data processing was performed using HP ChemStation software (rev. A.09.03 [1417]). In some cases, spectra were obtained from M-Scan Inc. (West Chester, PA). UV spectra were recorded on an Agilent 8453 UV–visible spectroscopy system from 200 to 500 nm. NMR spectra of AMBA, Lu-AMBA, and Hf-AMBA were acquired on a Bruker Avance III Ultra Shield Plus 600 MHz spectrometer using 1.3 mM solutions at pH 5 in  $\text{H}_2\text{O}$  (10%  $\text{D}_2\text{O}$ ) and at 300 K.  $^{13}\text{C}$  spectra were acquired on 10 mM solutions, although the Hf complex appeared to be less soluble than the peptide or Lu complex and tended to precipitate. NOESY spectra were acquired at 278 K to increase the NOE effect. A mixing time of 100 ms was used to avoid spin diffusion. The shifts were referenced to internal TSP.

**Synthesis of  $^{nat}\text{Lu-AMBA}$ .**  $\text{LuCl}_3 \cdot 6\text{H}_2\text{O}$  (14 mg, 0.036 mmol, 1.5 eq.) was added to AMBA (36.5 mg, 0.024 mmol, 1 equiv) dissolved in 5 mL of a 0.2 M NaOAc buffer, at pH 4.5. The resulting solution was refluxed for 15 min, cooled to room temperature, and purified using HPLC method 4. The fractions containing the peak of interest were pooled and lyophilized to yield 38 mg (75%) of Lu-AMBA  $\cdot 2\text{TFA} \cdot 10\text{H}_2\text{O}$  as a white solid. Anal. calcd for Lu-AMBA  $\cdot 2\text{TFA} \cdot 10\text{H}_2\text{O}$ : C, 41.52; H, 5.71; N, 12.78; S, 1.54 F, 5.47. Found: C, 41.18; H, 5.55; N, 12.62; S, 1.28 F, 5.19. Amino acid analyses calculated for Lu-AMBA: Gln 1, Gly 2, Ala 1, Val 1, Met 1, Leu 1, His 1, Trp 1. Found: Gln 1.05, Gly 2.18, Ala 1.06, Val 1.06, Met 1.06, Leu 1.08, His 1.06, Trp 0.44. ESI MS ( $m/z$ ): 1675.4  $[\text{M} + \text{H}]^+$ , 849.9  $[\text{M} + \text{H} + \text{Na}]^{2+}/2$ , 838  $[\text{M} + 2\text{H}]^{2+}/2$ .

**Synthesis of  $^{177}\text{Lu-AMBA}$ .** The synthesis of  $^{177}\text{Lu-AMBA}$  was performed as described previously.<sup>5</sup> Briefly, AMBA (120  $\mu\text{g}$ ,  $\sim 1.6$  equiv) was dissolved in 1 mL of 0.2 M NaOAc at pH 4.8 and mixed with  $\sim 2.22$  GBq of  $^{177}\text{LuCl}_3$  (in 0.05 N HCl, specific activity 103.6–151.3 GBq/ $\mu\text{mol}$ ). The mixture was heated at 100  $^{\circ}\text{C}$  in a heating block for 10 min and cooled to ambient temperature in a water bath for  $\sim 2$  min, and 2 mL of a 9:1 (v/v) mixture of bacteriostatic 0.9% sodium chloride injection USP and ASCOR L500 ascorbic acid injection USP (McGuff) was added to stabilize the product against radiolysis. The final product had a RCP of  $>94\%$ .

**$^{nat}\text{Lu}/^{177}\text{Lu}$  Coinjection Studies.** A 30  $\mu\text{L}$  aliquot of a solution prepared by dissolving 300  $\mu\text{g}$  of  $^{nat}\text{Lu-AMBA}$  in a 9:1 mixture of bacteriostatic saline/Ascor L500 was mixed with 13.2  $\mu\text{L}$  (14.3 MBq) of  $^{177}\text{Lu-AMBA}$  and 258  $\mu\text{L}$  of a 9:1 mixture of bacteriostatic saline/Ascor L500. The mixture was analyzed by HPLC using methods 1 (at 1 mL/min) and 2. The UV signal was recorded at 280 nm.

**Decay Experiment.**  $^{177}\text{Lu-AMBA}$  (20 mCi) was purified (HPLC method 6) to remove all unmetallated AMBA ligand. Fractions were collected into a radiostabilizer solution of 9:1 bacteriostatic saline/Ascor L500 that contained 2 mg/mL of Se-Met. The mixture was evaporated for 1 h in a speed vacuum to remove organic solvents. Purified Lu-AMBA (621 MBq, 16.8 mCi), with an initial specific

activity of 135.42 GBq/ $\mu\text{mol}$  and initial RCP of 94.3%, was stored at  $-20\text{ }^{\circ}\text{C}$  in a 1 mL volume and reanalyzed by HPLC after 42 days (6.4 half-lives) using  $\gamma$  and UV detection ( $A_{280}$ ). The relative areas under the UV peaks for the remaining Lu-AMBA and decay product (Hf-AMBA) were determined by integration. An aliquot (800  $\mu\text{L}$ ) of the decayed solution was purified using HPLC method 5, which provides excellent separation between Hf-AMBA (retention time,  $t_{\text{R}} = 19.2$  min) and Lu-AMBA ( $t_{\text{R}} = 20.4$  min). The fractions containing  $^{177}\text{Hf-AMBA}$  were pooled, lyophilized, and shipped to M-Scan for MALDI-MS; analysis yielded an isotopic pattern (base peak 1675.3 amu) consistent with  $^{177}\text{Hf-AMBA}$ .

**Synthesis of  $^{nat}\text{Hf-AMBA}$ .**  $\text{HfCl}_4$  (71.96 mg, 0.225 mmol, 15.1 equiv) was added to AMBA (29.7 mg, 0.0149 mmol, 1 equiv) dissolved in 30 mL of dry DMF. The resulting solution was heated at 110  $^{\circ}\text{C}$  in an oil bath for 1 h, cooled at room temperature, and filtered, and  $\text{Et}_2\text{O}$  (50 mL) was added with stirring. The white precipitate formed was washed with  $\text{Et}_2\text{O}$  (5 mL) and dried under a vacuum. The solid was redissolved in  $\text{H}_2\text{O}$  and purified using HPLC method 1; gradient elution showed the product to be comprised of two closely eluting peaks in a  $\sim 1:1$  ratio. The fractions of interest were pooled and lyophilized to yield 11.1 mg of Hf-AMBA  $\cdot 3\text{TFA} \cdot 6\text{H}_2\text{O}$  (38% based on a purity of 96%), as determined by HPLC method 2. Anal. calcd for Hf-AMBA  $\cdot 3\text{TFA} \cdot 6\text{H}_2\text{O}$ : C, 41.71; H, 5.25; N, 12.50; F, 8.45. Found: C, 41.78; H, 4.92; N, 11.97; F, 8.22. ESI MS ( $m/z$ ): 1678.4  $[\text{M} + \text{H}]^+$ , 839.6  $[\text{M} + 2\text{H}]^{2+}/2$ .

**Hf-AMBA Isomer Interconversion and Coinjection Studies.** The two peaks in Hf-AMBA were separated by HPLC (method 3), reduced in volume for 2 h in a speed vacuum, and reinjected at  $t = 0$  (after evaporation) and at 5 h intervals up to 70 h. Coinjection studies were performed by mixing authentic Hf-AMBA with an aliquot of decayed  $^{177}\text{Lu-AMBA}$ , followed by HPLC analysis ( $A_{280}$ ).

**Extinction Coefficient Determinations.** Lu-AMBA (0.172 mg) was dissolved in 0.864 mL of 0.1% TFA in  $\text{H}_2\text{O}$  to achieve a final concentration of  $1 \times 10^{-5}$  M. Hf-AMBA (0.185 mg) was dissolved in 0.868 mL of 0.1% TFA in  $\text{H}_2\text{O}$  to achieve a final concentration of  $1 \times 10^{-5}$  M. UV/vis spectra of the two solutions were recorded. Molar absorptivity  $\epsilon$  was calculated from the Beer–Lambert law [ $A = \epsilon bc$ ] and found to be 22 200  $\text{L mol}^{-1} \text{cm}^{-1}$ , with  $\lambda_{\text{max}} = 271$  nm (Lu-AMBA), and 21 400  $\text{L mol}^{-1} \text{cm}^{-1}$  (Hf-AMBA), with  $\lambda_{\text{max}} = 271$  nm.

## Results

**Synthesis of  $^{nat}\text{Lu-AMBA}$ .** Lu-AMBA (Figure 1), isolated as its bis trifluoroacetate salt, was readily prepared by heating excess  $\text{LuCl}_3 \cdot 6\text{H}_2\text{O}$  with AMBA in a 0.2 M NaOAc buffer, at pH 4.5 for 15 min at 100  $^{\circ}\text{C}$ . The results of elemental and moisture analyses are consistent with the calculated values. Good correlation was obtained between the theoretical amino acid sequence G-Abz4-QWAVGHLM-NH<sub>2</sub> (Abz4 = 4-aminobenzoyl) and observed values for all amino acids except tryptophan, which is known to yield low values due to degradation of the tryptophan residue during acid hydrolysis. The molecular formula of Lu-AMBA was confirmed by mass spectroscopy.

**HPLC Coinjection of  $^{nat}\text{Lu-AMBA}$  and  $^{177}\text{Lu-AMBA}$ .** The preparation of  $^{177}\text{Lu-AMBA}$  and methods for stabilizing it against radiolytic damage from the  $\beta^-$  emissions of the  $^{177}\text{Lu}$  radioisotope have been reported previously.<sup>5</sup> The results of HPLC coinjection studies with  $^{nat}\text{Lu-AMBA}$  and  $^{177}\text{Lu-AMBA}$

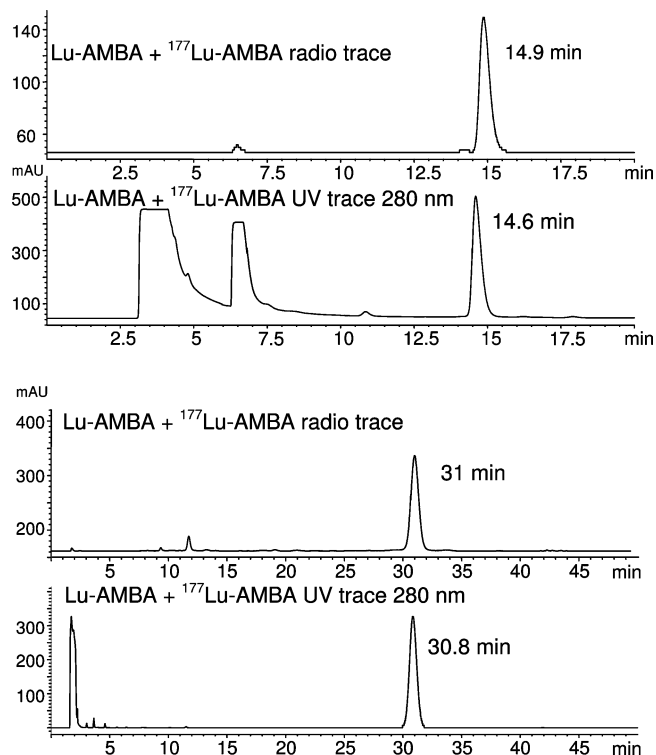


**Figure 2.** Coinjection of <sup>175</sup>Lu-AMBA and <sup>177</sup>Lu-AMBA in two different HPLC systems. <sup>177</sup>Lu-AMBA had a retention time of ~14.9 min using HPLC method 4, and a *t<sub>r</sub>* of 31 min when analyzed using HPLC method 2. The difference in retention times of corresponding UV and radiochromatograms is due to the offset of the two detectors.

AMBA (Figure 2) demonstrate the equivalence of the radioactive <sup>177</sup>Lu-AMBA complex and the nonradioactive Lu-AMBA standard in two different HPLC systems. The early peaks in the UV chromatograms for <sup>177</sup>Lu-AMBA are due to formulation components such as Ascor, benzyl alcohol, EDTA, and selenomethionine. The ~0.2 min difference in retention time between the UV signal and the radio signal is due to the dead volume between the two detectors.

**Synthesis of Hf-AMBA.** An authentic sample of Hf-AMBA was prepared by heating anhydrous HfCl<sub>4</sub> and AMBA in dry DMF for 1 h. After HPLC purification, the resulting product provided elemental analysis results that were consistent with its formulation as Hf-AMBA·3TFA·6H<sub>2</sub>O. The molecular formula of Hf-AMBA was confirmed by ESI-MS (*m/z*): 1678.4 [M + H]<sup>+</sup>, 839.6 [M + 2H]<sup>2+</sup>/2.

**Hf-AMBA Interconversion Studies.** The two closely eluting UV peaks isolated from the synthesized <sup>nat</sup>Hf-AMBA showed slow interconversion over the course of ~70 h. At the end of the study (70 h), isolated peak 1 contained a 60:40 mixture of peak 1 and peak 2, whereas isolated peak 2 contained a 40:60 mixture of peak 1 and peak 2. Both peaks yielded the same mass spectra by LC-ESI-MS, further demonstrating that they are a pair of Hf-AMBA isomers, the nature of which have not been clarified.

**<sup>177</sup>Hf-AMBA in Decayed Solutions of Purified <sup>177</sup>Lu-AMBA.** HPLC traces obtained after the decay of purified <sup>177</sup>Lu-AMBA (~16.8 mCi in ~1 mL of a radiostabilizing solution) are shown in Figure 3. After 42 days of storage at -20 °C (~6.4 half-lives), the remaining <sup>177</sup>Lu-AMBA (now

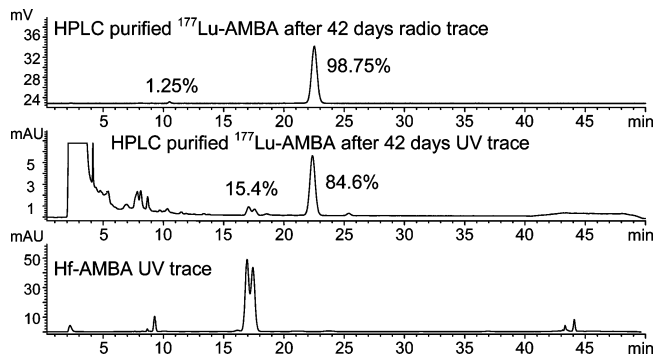


**Figure 3.** Top panel: Radiochromatogram of <sup>177</sup>Lu-AMBA (retention time 22.5 min) after 42 days of decay at -20 °C. The small (1.25%) peak at 10.5 min is an oxidation product of <sup>177</sup>Lu-AMBA, wherein the terminal methionine-amide has been oxidized to methionine oxide. Middle panel: UV trace (*A*<sub>280</sub>) of decayed solution. Bottom panel: UV trace of authentic sample of Hf-AMBA. The doublet in this trace coelutes with the doublet found in decayed solutions of <sup>177</sup>Lu-AMBA. HPLC method, Agilent/Zorbax Bonus RP column (250 × 4.6 mm, 5 μm silica) eluted as follows: from 30% 30 mM (NH<sub>4</sub>)<sub>2</sub>SO<sub>4</sub> in H<sub>2</sub>O with 0.1% TFA (v/v)/60% H<sub>2</sub>O/5% MeOH/5% ACN to 12/60/14/14 in 5 min; hold at 12/60/14/14 for 35 min, ramp to 0/60/20/20 in 3 min; hold at 0/60/20/20 for 5 min, return to 30/60/5/5 in 1 min. Flow rate: 1.5 mL/min, *T* = 37 °C.

~0.2 mCi) had a RCP of >98%, indicating that the stabilizing solution effectively prevented radiolytic damage to the remaining Lu-AMBA. No radioactivity was found at the void volume, indicating that no free <sup>177</sup>Lu<sup>3+</sup> had formed, and no peaks for unmetallated AMBA ligand were detected.

The UV trace for the decayed <sup>177</sup>Lu-AMBA solution showed the expected decrease in peak area of the <sup>177</sup>Lu-AMBA peak (Lu-AMBA *t<sub>R</sub>* = 22.5 min) and a similar increase in the area of a new nonradioactive doublet peak with *t<sub>R</sub>* = 17.5 min. In Figure 3, the HPLC trace of the decayed <sup>177</sup>Lu-AMBA (middle panel) is compared to that of <sup>nat</sup>Hf-AMBA (bottom panel). The retention times of the two peaks in authentic Hf-AMBA were identical to those of the new nonradioactive doublet peak in the decayed solution of purified <sup>177</sup>Lu-AMBA.

The decay product was further identified by MALDI-MS. The expected isotope pattern and *m/z* (1675.3) for <sup>177</sup>Hf-AMBA were observed in the MALDI-MS spectrum of the isolated decay product. In Figure 4, the actual and theoretical mass spectra of an authentic sample of <sup>nat</sup>Hf-AMBA are compared with those of the <sup>177</sup>Hf-AMBA isolated from the solution of decayed <sup>177</sup>Lu-AMBA. As expected, <sup>nat</sup>Hf contains a mixture of six Hf isotopes (<sup>174</sup>Hf, <sup>176</sup>Hf, <sup>177</sup>Hf, <sup>178</sup>Hf, <sup>179</sup>Hf, and <sup>180</sup>Hf in a 0.16:5.3:18.6:27.3:13.6:31.1 ratio), whereas <sup>177</sup>Hf-AMBA, formed via the decay of <sup>177</sup>Lu-AMBA, contains only <sup>177</sup>Hf.

**NMR Results.** The <sup>1</sup>H and <sup>13</sup>C NMR spectra of AMBA, Lu-AMBA, and Hf-AMBA 1.3 mM at pH 5 in H<sub>2</sub>O (10% D<sub>2</sub>O) and 300 °K are shown in Figures 5 and 6. Almost complete <sup>1</sup>H and <sup>13</sup>C assignment was accomplished by a series of 2D spectra, namely, 2D-NOESY, 2D-COSY, 2D-TOCSY-<sup>1</sup>H, <sup>13</sup>C-HSQC, 2D-<sup>1</sup>H, <sup>13</sup>C-HSQC, 2D-<sup>1</sup>H, and <sup>13</sup>C-HMBC. The <sup>1</sup>H and <sup>13</sup>C assignments and <sup>HN-HA</sup>*J* coupling constants for the AMBA ligand and its Lu and Hf complexes are reported in Tables S1–6 (Supporting Infor-

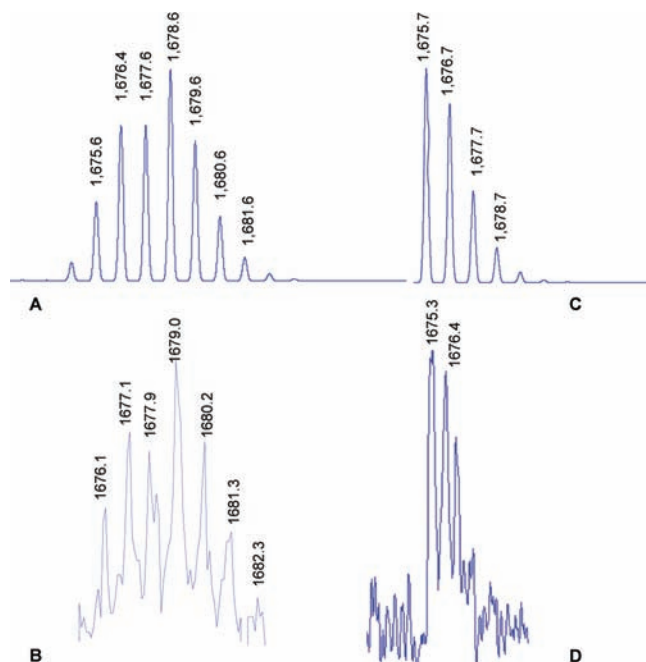


**Figure 4.** Calculated (panel A) and observed (panel B) electrospray mass spectra of  $^{\text{nat}}\text{Hf-AMBA}$  and the calculated (panel C) and observed (panel D) MALDI spectra of  $^{177}\text{Hf-AMBA}$  isolated from decayed  $^{177}\text{Lu-AMBA}$  solution. The spectra are different because natural Hf contains several Hf isotopes, whereas  $^{177}\text{Hf-AMBA}$  formed from the decay of  $^{177}\text{Lu-AMBA}$  only contains  $^{177}\text{Hf}$ .

mation). On the basis of NMR studies, the solution structures of the AMBA ligand (Figure 7) and its complexes were determined. Key NOE data are shown in Figure 4S (Supporting Information). A minimized structure for the metal complex obtained independently from NOE constraints is shown in Figure 8.

The complexity of the proton signals of the DO3A chelator demonstrates the presence of multiple conformations in intermediate exchange, as demonstrated by their large linewidths. For this reason, their assignments are only tentative and reflect the main species. NMR spectra for Hf-AMBA in areas corresponding to resonances from the DO3A chelator are narrower but significantly more complex than those found for Lu-AMBA and the unmetallated ligand, reflecting the presence of multiple species in Hf-AMBA. The NMR data for Hf-AMBA support its formulation as a Hf(IV) complex, as shifts expected if the metal was paramagnetic Hf(III) were not observed.

## Discussion

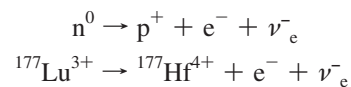
**Decay Experiment.** In the present experiments, the  $^{177}\text{LuCl}_3$  isotope source used was prepared from an enriched  $^{176}\text{Lu}$  target, so the isotope source contained a significant amount of  $^{176}\text{Lu}$  carrier.<sup>11,14</sup> On the date and time that the synthesis and HPLC purification of  $^{177}\text{Lu-AMBA}$  was performed, the specific activity of the starting Lu-AMBA was 135.42 GBq/ $\mu\text{mol}$ . It can be calculated that, for this lot of  $^{177}\text{Lu}$ , only 18.9% of the total Lu ( $^{175}\text{Lu} + ^{176}\text{Lu} + ^{177}\text{Lu}$ ) was present as  $^{177}\text{Lu}$ ; the remainder (81.1%) was  $^{175/176}\text{Lu}$ ,

the target material used to prepare the  $^{177}\text{Lu}$ . If no radiolytic damage occurs, the amount of  $^{175/176}\text{Lu-AMBA}$  that is present should not change over time, but the relative amount of  $^{177}\text{Lu-AMBA}$  will fall as  $^{177}\text{Lu}$  decays to  $^{177}\text{Hf}$ .

The fraction of  $^{177}\text{Lu}$  remaining after 42 days of decay is equal to  $e^{-kt}$ , where the decay constant ( $k$ ) =  $0.693/t_{1/2}$  of  $^{177}\text{Lu}$  and  $t$  is the time elapsed. Making the proper substitutions for  $t_{1/2}$  (6.7 days), elapsed time (42 days), and  $^{177}\text{Lu}$  decay constant  $k$  ( $0.1034 \text{ d}^{-1}$ ), the percentage of the initial  $^{177}\text{Lu}$  remaining is  $\exp[-\ln(2)/6.7] \times 42 \text{ days} \times 100 = 1.2\%$ , indicating a 98.8% conversion to  $^{177}\text{Hf}$ . Thus, the fraction of the  $t = 0$  Lu-AMBA UV area that was due to  $^{177}\text{Lu-AMBA}$  (18.9%) should decrease by 98.8% (to 0.2%) due to its decay to  $^{177}\text{Hf}$ , regardless of the product(s) that are formed. If 98.7% of the  $^{177}\text{Lu-AMBA}$  initially present was converted quantitatively to  $^{177}\text{Hf-AMBA}$ , and the final Hf product has the same extinction coefficient as the starting Lu-AMBA, the relative areas under the UV peaks for the Hf-AMBA and Lu-AMBA peaks should be as calculated in Table 1. This approximation can be safely made, as the extinction coefficients at 271 nm for Lu-AMBA and Hf-AMBA were found to be  $2.22 \times 10^4$  and  $2.14 \times 10^4 \text{ M}^{-1} \text{ cm}^{-1}$ , respectively.

When the peaks corresponding to  $^{177}\text{Hf-AMBA}$  and  $^{177/176/175}\text{Lu-AMBA}$  in the decayed Lu-AMBA solution were integrated, the area percent under the  $^{177}\text{Hf-AMBA}$  peaks and  $^{177/176/175}\text{Lu-AMBA}$  peak were 15.4% and 84.6%, respectively. The amount of  $^{177}\text{Hf-AMBA}$  formed, on the basis of the UV area under the new nonradioactive peaks, was 82.5% of that predicted, on the basis of the amount of Lu-AMBA that had decayed [15.4% (observed), 18.7% (calculated)]. Finally, the decay product was found to coelute with authentic samples of  $^{\text{nat}}\text{Hf-AMBA}$  and to have the expected molecular weight (1675) using mass spectrometry. Thus, the molecular weight, integrated peak areas, and retention times of the new products in decayed  $^{177}\text{Lu-AMBA}$  and the coelution of authentic Hf-AMBA with the  $^{177}\text{Lu-AMBA}$  decay product peaks all support the conclusion that the new doublet observed was  $^{177}\text{Hf-AMBA}$ .

**Oxidation State of Hf-AMBA.** During  $\beta^-$  decay, a neutron ( $n^0$ ) in the parent isotope is converted into a proton ( $p^+$ ) while an electron ( $e^-$ ) and an antineutrino ( $\bar{\nu}_e$ ) are emitted.  $^{177}\text{Lu}$ , which has 71 protons, is converted to  $^{177}\text{Hf}$ , which has 72. The overall charge of the metal increases by +1 as a consequence of the  $\beta^-$  decay process.



The resulting product, if the decay process does not destroy or damage the molecule, would be  $^{177}\text{Hf(IV)-AMBA}$ . The elemental analysis results for Lu-AMBA and Hf-AMBA were consistent with oxidation of the central metal from +3 to +4, as the two complexes were isolated as bis- and tris-TFA salts, respectively. The retention time of the new Hf-containing product, which is more polar than the starting Lu-AMBA, is also consistent with the proposed formulation. The NMR is also

(14) Pillai, M. R.; Chakraborty, S.; Das, T.; Venkatesh, M.; Ramamoorthy, N. *Appl. Radiat. Isot.* **2003**, *59* (2–3), 109–118.

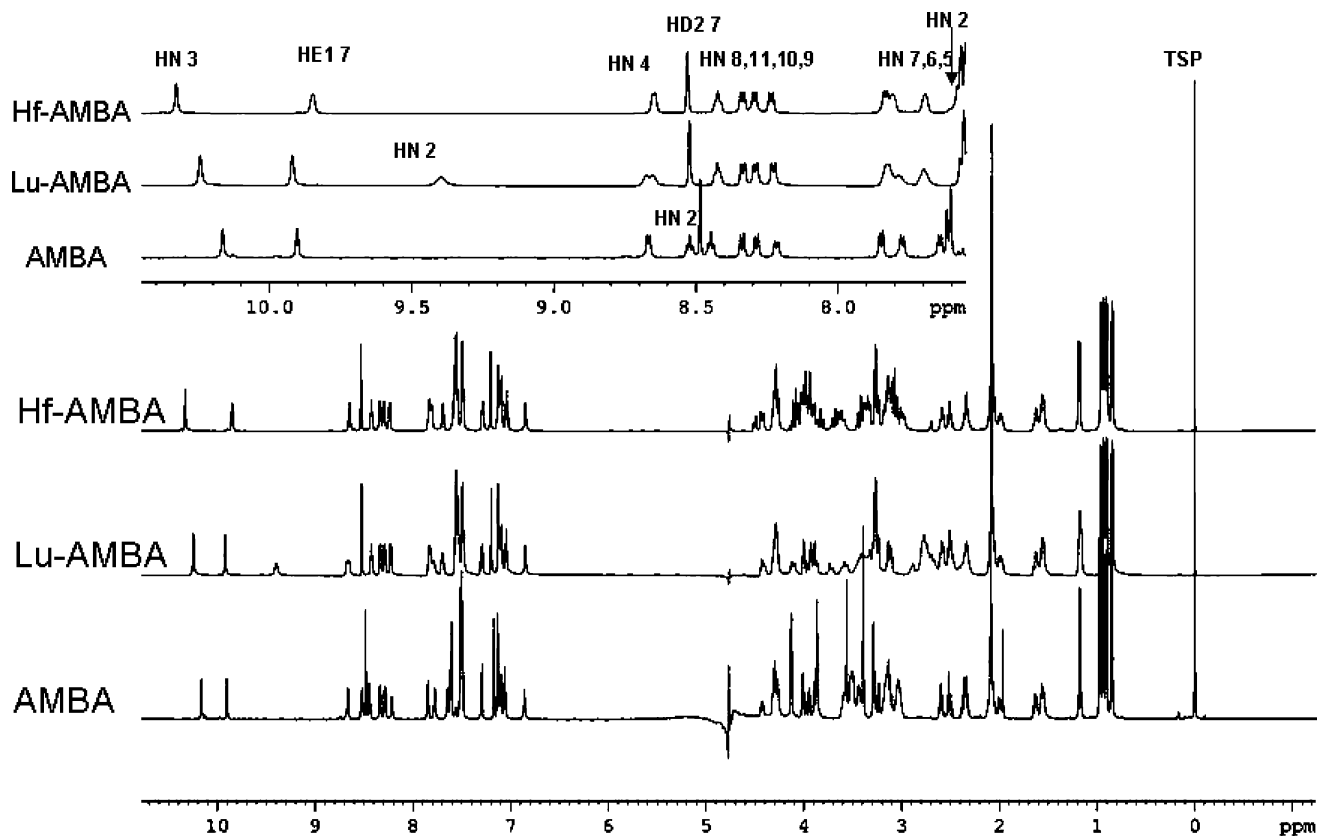


Figure 5. <sup>1</sup>H spectra of AMBA (1.3 mM) and its Lu and Hf complexes at pH 5 in H<sub>2</sub>O (10% D<sub>2</sub>O), 300 ° K.

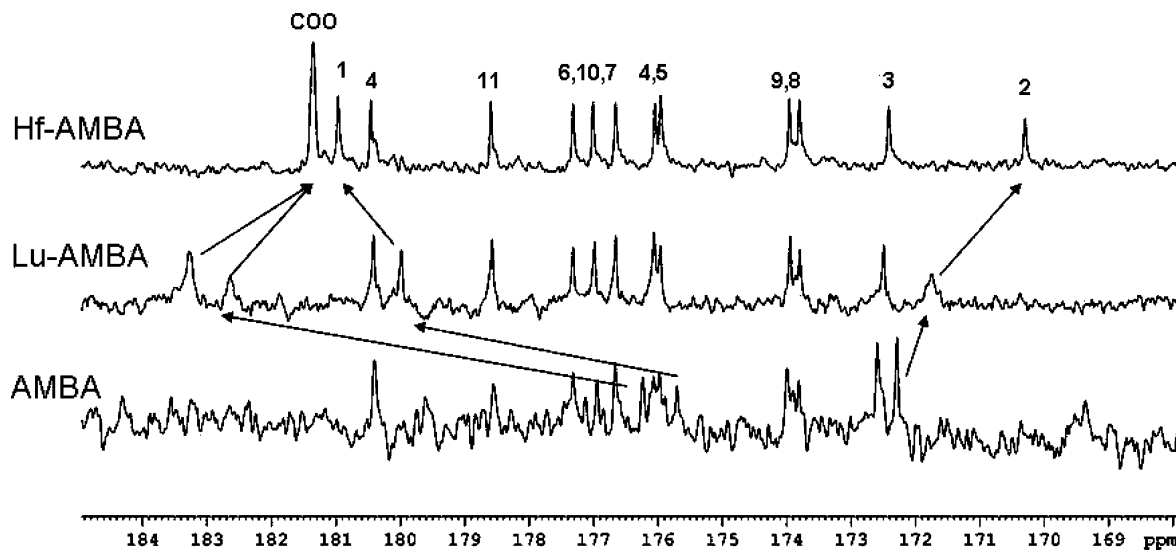


Figure 6. <sup>13</sup>C spectra of AMBA and its Lu and Hf complexes (carbonyl region). Carbonyl atoms of residues 1 and 2 (and the DO3A carboxylates) experience significant shift upon metal complexation.

consistent with a Hf(IV) complex, since a Hf(III) complex would be expected to be paramagnetic and its spectrum would display much larger linewidths.

Hf(III) has no known aqueous chemistry due to its ability to reduce water.<sup>15</sup> The +4 oxidation state of Hf is very stable, due to its d<sup>0</sup> electron configuration. Hafnium(IV)

complexes with aminocarboxylate ligands like ethylene dioxydiethylenedinitrilotetracetic acid<sup>16</sup> and EDTA<sup>17</sup> have been reported.

Despite the stability of Hf(IV) aminocarboxylate complexes once formed, in-house studies (unpublished results) have demonstrated that Hf(IV)Cl<sub>4</sub> solutions do not react with DO3A-containing chelators such as AMBA under the aqueous conditions used to prepare <sup>177</sup>Lu-AMBA. As a result, the presence of “free” <sup>177</sup>Hf(IV) in radiolabeling solutions

(15) Greenwood, N. N.; Earnshaw A. *Chemistry of the Elements*; Pergamon Press Ltd.: Oxford, England, 1984; p 1117.

(16) Evans, D. F.; Griffiths, G. W.; O’Mahoney, C.; Williams, D. J.; Wong, C. Y.; Woolins, J. D. *J. Chem. Soc., Dalton Trans.* **1992**, 2475–2479.

(17) Aochi, Y. O.; Sawyer, D. T. *Inorg. Chem.* **1966**, 5 (12), 2085–2092.

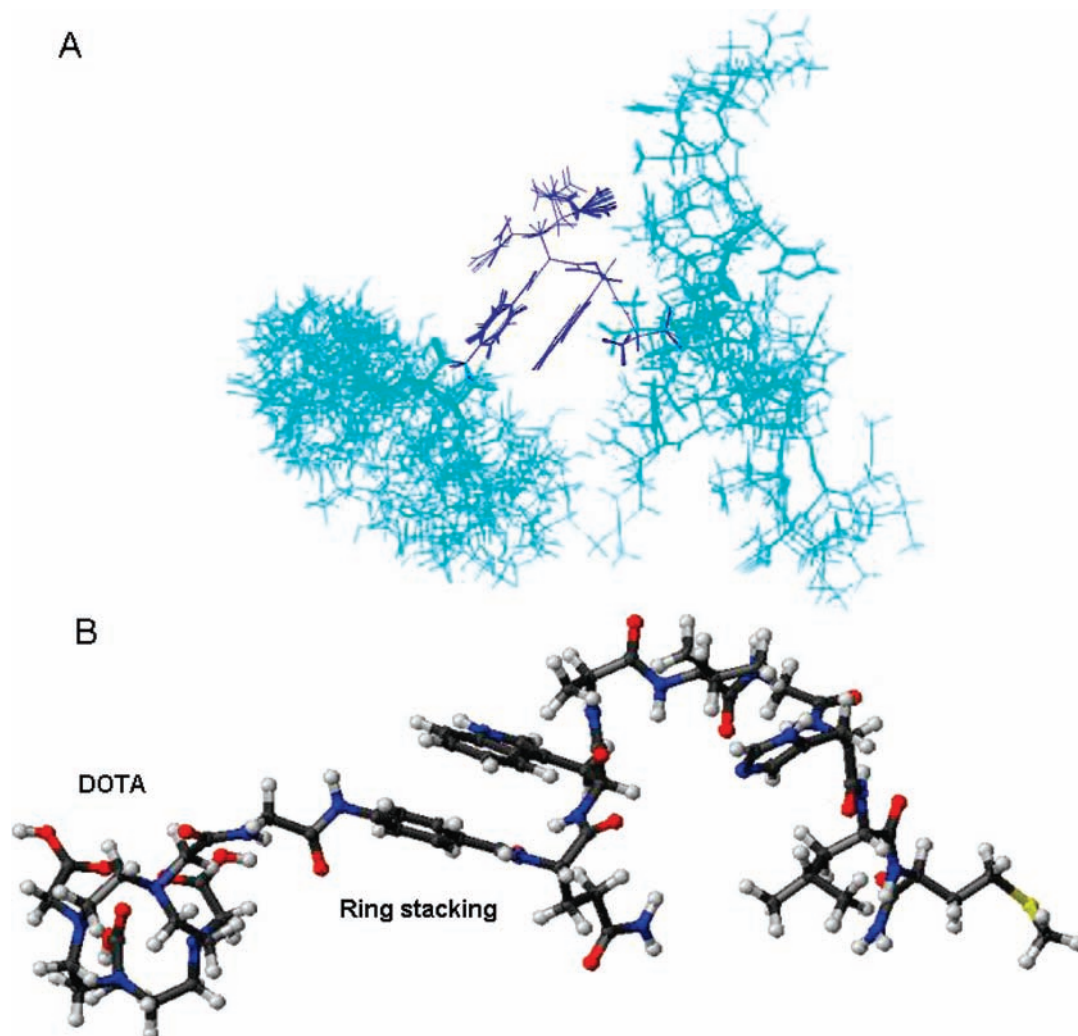


**Figure 7.** Solution structure of uncomplexed AMBA at pH 5, 278 K. (A) Family of structures obtained by fitting the positions of the atoms in the region between the aminobenzoyl moiety and alanine residue. (B) Selected structure within the family showing the ring stacking between the aromatic rings of the linker and the tryptophan residue.

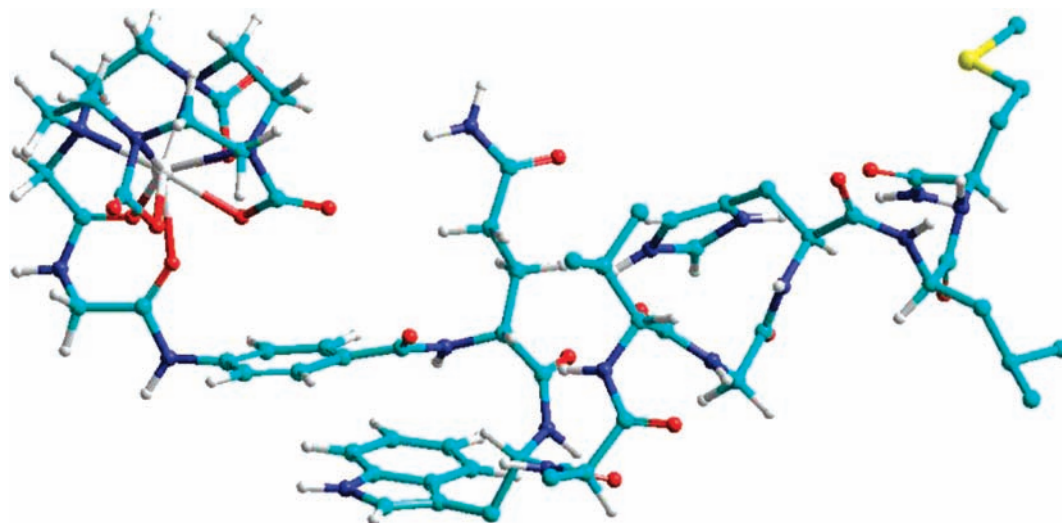


**Figure 8.** Minimized structure of M-AMBA complex.

does not compete for ligands during the preparation of  $^{177}\text{Lu}$ -AMBA. Similarly, Breeman et al.<sup>12</sup> have reported that Hf(IV) does not interfere with the  $^{177}\text{Lu}$  labeling of  $^{177}\text{Lu}$ -octreotate. In aqueous acidic (HCl, HClO<sub>4</sub>, and CF<sub>3</sub>SO<sub>3</sub>H) solutions,

Hf(IV)Cl<sub>4</sub> is hydrolyzed readily, forming a mixture of polymeric adducts containing OH<sup>-</sup> and H<sub>2</sub>O, dependent on the acid strength. The hydrolysis product of hafnium(IV) in perchloric acid has been found to be the unreactive polymer

**Table 1.** Relative Areas under the UV Peaks for Hf-AMBA and Lu-AMBA

	<sup>177</sup> Hf	<sup>177</sup> Lu	<sup>175/176</sup> Lu
calculated ( <i>t</i> = 0)	0	18.9%	81.1%
calculated ( <i>t</i> = 42 d)	18.7%	0.2%	81.1%
found ( <i>t</i> = 42 d)	15.4%	<sup>177</sup> Lu + <sup>175/176</sup> Lu = 84.6%	

[Hf<sub>4</sub>(OH)<sub>8</sub>(H<sub>2</sub>O)<sub>16</sub>]<sup>8+</sup>, often labeled HfO(2+)·5H<sub>2</sub>O.<sup>18</sup> X-ray scattering studies of HfOCl<sub>2</sub>·8H<sub>2</sub>O (isolated from 6N HCl) show it to be a tetrameric complex [Hf<sub>4</sub>(OH)<sub>8</sub>(H<sub>2</sub>O)<sub>16</sub>]Cl<sub>8</sub> with the Hf metal atoms arranged in a square and held together by double OH bridges along each edge.<sup>19</sup> This tendency to form unreactive OH-bridged polymers may explain our failure to synthesize Hf(IV) complexes of AMBA under aqueous conditions. Although the nature of the Hf(IV) species present in aqueous acetate buffer has not been reported, Hf(OAc)<sub>4</sub> is not known. Therefore the species present are likely to have some polymeric character.

Although Hf-AMBA could not be formed in water, we were successful in preparing an authentic sample of Hf-AMBA from the reaction of anhydrous HfCl<sub>4</sub> with AMBA in dry DMF. To our knowledge, this is the first reported synthesis of a Hf-DO3A monoamide derivative. The reactivity of HfCl<sub>4</sub> with AMBA was also tested in MeOH, EtOH, and isopropanol. As was found in H<sub>2</sub>O, the reactions in EtOH and isopropanol yielded no product, but the reaction in dry MeOH produced Hf-AMBA in good yield. As was found in the sample of <sup>177</sup>Hf-AMBA formed by the decay of <sup>177</sup>Lu-AMBA, the authentic standard of Hf-AMBA was two slowly interconverting species, both of which had the same molecular weight. Although NMR studies clearly show that they are both conjugates of the DO3A-monoamide-containing AMBA ligand, the exact natures of the two species require further study. It is very possible that they are conformational isomers, as it is well-known that macrocyclic metal-(DOTA) derivatives exist in solution as a mixture of compounds differing in ligand conformation, namely, square antiprismatic and twisted square antiprismatic geometries. Which conformation is favored has been shown to depend on the nature of the central metal and on the substituents present on the chelator.<sup>3,20–22</sup>

The possibility also exists that the interconverting species are isomers wherein the peptide portion of the molecule is cis or trans relative to the coordinated amide carbonyl, as found previously in Y(III)-DOTATATE.<sup>36</sup> However, the NMR evidence does not support this possibility, as we do not observe any doubling of resonances at the level of the amide protons in the Hf complex. The complexity in the Hf complex is strictly confined in the DOTA region. Note that we do observe a doubling of the amide at the level of the Gln residue, but only in the Lu complex.

**Comparison to Previous Results.** Our ability to isolate >80% of decayed <sup>177</sup>Lu-AMBA as an intact <sup>177</sup>Hf-AMBA complex is unusual, as the radioactive decay process is frequently catastrophic for the molecule that undergoes decay. As noted in an excellent review by Halpern and Stöcklin,<sup>13</sup> there are four potential sources of chemical excitation following β<sup>-</sup> decay that have the potential to damage a molecule. These include effects due to the change of the chemical identity, the positive charge imparted to the daughter atom, mechanical recoil due to conservation of momentum, and electronic excitation due to a sudden change of *Z*. These factors can have greater or lesser importance depending on the radionuclide, emission type, emission energy, and chemical bonds involved. The change in chemical identity and the positive charge that the daughter atom obtains after decay frequently lead to molecular fragmentation, as the resulting compound is not chemically stable. Usually, these effects cause the rupture of the bond bearing the daughter atom, but they can also have secondary consequences, such as the formation of new chemical bonds. For example, Jiang et al.<sup>23</sup> studied the decay of <sup>131</sup>I in aqueous solutions of *o*-iodophenol doubly labeled with <sup>131</sup>I and <sup>14</sup>C and found that the primary effect was the conversion of the aromatic C–<sup>131</sup>I bond to –C–OH.

**Recoil from β<sup>-</sup> (Electron) Emitted during Decay.** Recoil energy upon emission of radiation can give rise to damage to the local environment of the daughter nuclide. If the recoil energy is high enough, chemical bonds can be broken. Recoil is very high for radionuclides that emit α particles (He<sup>2+</sup>), due to the large size and high energy (3–7 MeV) of the particle emitted. Recoil energy is lower for β<sup>-</sup> emitters, due to the low mass of the electron, and varies depending on the energy *E*<sub>β</sub> of the emitted electron. The recoil energy of a daughter atom is given by the following equation, based on laws of conservation of momentum:<sup>13</sup>

$$E_R = \frac{m_0(E_\beta + 1.02)}{0.5} \cdot \frac{E_\beta}{2M} \quad (1)$$

which can be written numerically as

$$E_R(\text{in eV}) = \frac{536}{M} [E_\beta^2 + 1.02E_\beta] \quad (1a)$$

where *E*<sub>β</sub> is the energy of a β<sup>-</sup> particle in megaelectron volts (MeV), *m*<sub>0</sub> is the rest mass of the electron, and *M* is the mass of the recoil atom in amu.

Charge buildup can also lead to catastrophic consequences—this is particularly true for compounds labeled with <sup>125</sup>I, the decay of which can lead to the emission of 5–30 Auger electrons,<sup>13,24</sup> leaving very high net charges on the daughter. In general, decomposition of the immediate decay product is observed. For example, the major products formed following the radioactive decay of <sup>125</sup>I in [2-<sup>14</sup>C,5-<sup>125</sup>I]iodouracil<sup>25</sup> were found to be <sup>14</sup>CO and <sup>14</sup>CO<sub>2</sub>. Likewise, when the decay of

(18) Hagfeldt, C.; Kessler, V.; Persson, I. *Dalton Trans.* **2004**, *14*, 2142–2151.

(19) Muha, G. M.; Vaughan, P. A. *J. Chem. Physics.* **1960**, *33* (1), 194–199.

(20) Benetollo, F.; Bombieri, G.; Calabi, L.; Aime, S.; Botta, M. *Inorg. Chem.* **2003**, *42* (1), 148–157.

(21) Cosentino, U.; Villa, A.; Pitea, D.; Moro, G.; Barone, V.; Maiocchi, A. *J. Am. Chem. Soc.* **2002**, *124* (17), 4901–4909.

(22) Ranganathan, R. S.; Raju, N.; Fan, H.; Zhang, X.; Tweedle, M. F.; Desreux, J. F.; Jacques, V. *Inorg. Chem.* **2002**, *41* (25), 6856–6866.

(23) Jiang, V. W.; Krohn, K. A.; Welch, M. J. *J. Am. Chem. Soc.* **1975**, *97* (22), 6551–6556.

(24) Kassis, A. I.; Adelstein, J. S. *J. Nucl. Med.* **2005**, *46* (1), 4S–12S.

(25) Deutzmann, R.; Stoecklin, G. *Radiat. Res.* **1981**, *87* (1), 24–36.



$^{125}\text{I}$ -Tyr-labeled bungarotoxin was studied for up to  $10^{125}\text{I}$  half-lives, it was found that at least 95.3% of all radiolabeled bungarotoxin molecules were inactivated by the decay event.<sup>26</sup> Cols et al.<sup>27</sup> found that circular single-stranded DNA from the S13 phage, labeled with  $^{32}\text{P}$  or  $^{33}\text{P}$ , underwent systematic single strand break with each  $^{32}\text{P}$  decay (100%). For  $^{33}\text{P}$ , the lethal events were either a single strand break (40%) or a local stereochemical modification (33%) when the  $^{33}\text{P}$  of a phosphate decayed to sulfate.

For chelated radiometals, very few examples of the isolation of decay products have been reported. Glentworth and Betts<sup>28</sup> studied the decay products formed from the EDTA complex  $^{177}\text{Yb}(\text{EDTA})$ .  $^{177}\text{Yb}$  ( $t_{1/2} = 1.8$  h), which undergoes  $\beta^-$  decay to  $^{177}\text{Lu}$ , should form a stable EDTA complex as  $\text{Lu}(3+)$ . However, when the decayed solutions were analyzed, 59% of the resulting  $^{177}\text{Lu}$  had been lost from the EDTA chelator and was found in solution as unchelated  $^{177}\text{Lu}(3+)$ . Glentworth and Wright<sup>29</sup> compared the results obtained following the  $\beta^-$  decay of  $^{143}\text{Ce}(\text{DTPA})^{2-}$  and  $^{144}\text{Ce}(\text{DTPA})^{2-}$  and EDTA and DCTA analogs to their respective  $^{143}\text{Pr}$  and  $^{144}\text{Pr}$  complexes. A marked difference in the effects of  $\beta^-$  decay was observed for the two isotopes and for different chelators, with  $89 \pm 10\%$  breakup of the daughter complex produced by the  $\beta^-$  decay of  $^{143}\text{Ce}(\text{DTPA})^{2-}$ , compared to pH-dependent values of from  $30.9 \pm 1\%$  to  $66.3 \pm 5\%$  for the loss of the chelator following the decay of  $^{144}\text{Ce}(\text{DTPA})^{2-}$ . Sueki et al.<sup>30</sup> studied the stability of radiometal-loaded metallofullerenes following the decay of the radiometal. They found that, for the  $\beta^-$  decay of both  $^{155}\text{Sm} \rightarrow ^{155}\text{Eu}$  and  $^{161}\text{Gd} \rightarrow ^{161}\text{Tb}$  inside fullerenes, most of the  $^{155}\text{Eu}$  and  $^{161}\text{Tb}$  remained intact within the carbon cage of the parent nuclide. Interestingly, this was not true for the  $^{177}\text{Yb}$  that underwent  $\beta^-$  decay to  $^{177}\text{Lu}$ . The original metallofullerene became unstable and appeared to lose  $^{177}\text{Lu}$ , as radioactivity was not eluted at the expected HPLC retention time. Such a difference of the effect of  $\beta^-$  decay on the stability of metallofullerenes cannot be explained by the difference of recoil energies, because they are similar for all three of the decaying isotopes.

So what explains the fact that intact  $^{177}\text{Hf}$ -AMBA is found in decayed solutions of  $^{177}\text{Lu}$ -AMBA? We believe it is due to many factors, including the relatively low energy of the  $\beta^-$  emission ( $E_\beta$ ) from  $^{177}\text{Lu}$ , the oxidation state of the resulting  $^{177}\text{Hf}(4+)$ , and the nature of the DO3A chelator. The maximum recoil energy  $E_M$  generated from the decay of  $^{177}\text{Lu}$  to  $^{177}\text{Hf}$  can be calculated using the formula<sup>31</sup> shown in eq 2, where  $E_\beta$  is the maximum  $^{177}\text{Lu}$   $\beta^-$  energy in mega-electron volts (0.498 MeV) and  $M$  is the mass of the nuclide (177).

$$E_M (\text{eV}) = \frac{536}{M} E_\beta^2 + \frac{541}{M} E_\beta \quad (2)$$

It can be calculated that the maximum recoil energy for this decay process is 2.27 eV. The mean energy of  $\beta^-$  decay from  $^{177}\text{Lu}$ <sup>32</sup> is roughly 1/3 of the maximal value (0.149 MeV), which is, on average, lower than that of most chemical bond energies (2–6 eV). If the decaying atom is chemically bonded to other atoms, only a fraction of the recoil energy becomes available for bond rupture, the rest of it appearing as translational energy of the whole molecule.<sup>13</sup> In the local area where  $^{177}\text{Lu}$  decays to  $^{177}\text{Hf}$ , the bonds that could be broken are Hf–O; Hf–N; and adjacent C–N, C–H, and C–O bonds. Breaking of one or more metal–oxygen or metal–nitrogen bonds would not be expected to give rise to a loss of the metal due to the multidentate nature of the DO3A monoamide chelator, as many bonds would need to be broken simultaneously for the metal to be able to leave the chelator. In addition, the resulting  $\text{Hf}(4+)\text{DO3A}$  complex is in an oxidation state that is stable for Hf. The study was performed at  $-20$  °C in a stabilizing solution<sup>5</sup> that was designed to inhibit radiolytic damage due to the emitted  $\beta^-$  particles.

Our before-and-after-decay peak area analysis (280 nm absorbance) of purified  $^{177}\text{Lu}$ -AMBA, which is based on the similarity of extinction coefficients for  $^{\text{nat}}\text{Hf}$ -AMBA and  $^{\text{nat}}\text{Lu}$ -AMBA, indicates that  $\sim 15\%$  of the initial  $^{177}\text{Lu}$ -AMBA is unaccounted for. The nature of the product(s) that make up the remaining 15% of  $^{177}\text{Hf}$  that was not recovered is unknown at this time. There is the potential that the 15% “missing” product represents cumulative potential errors in the experiment. The starting 16.2 mCi of  $^{177}\text{Lu}$ -AMBA used in the decay experiment represents only 7.7  $\mu\text{g}$  of material. After decay, the UV area under the chromatographic peaks was very small, so there may be issues with the limit of quantitation or detector linearity in this range. In addition, errors in the initial determination of specific activity could lead to an over- or underestimation of expected yield. Minor amounts of product could be lost to oxidation of the peptide. The terminal residue of the AMBA ligand is an amidated methionine, which can be oxidized to its methionine sulfoxide analog if not properly radiostabilized.<sup>5</sup> As 1.25% of the original Lu-AMBA underwent such oxidation, the formation of a small percentage of Hf-AMBA methionine oxide is likely, but this peak, if present, would elute at an early retention time that would be hard to distinguish from stabilizer and solvent peaks. Finally, some Hf might dissociate from the AMBA ligand due to recoil, giving rise to a UV peak for the free ligand. The AMBA ligand has a retention time of 18 min in the system used for the decay studies, so the small peak that elutes just after  $^{177}\text{Hf}$  in Figure 3 may, in fact, be the free ligand.

**NMR Results.** After a careful examination of the  $^1\text{H}$  and TOCSY spectra for AMBA, all chemical shifts were assigned. They were further verified by reviewing COSY,

(26) Schmidt, J. J. *Biol. Chem.* **1984**, 259 (2), 1160–1166.

(27) Cols, P.; Apelgot, S.; Guille, E. *Radiat. Environ. Biophys.* **1988**, 27 (4), 261–275.

(28) Glentworth, P.; Betts, R. H. *Can. J. Chem.* **1961**, 39, 1049–1053.

(29) Glentworth, P.; Wright, C. L. *J. Inorg. Nucl. Chem.* **1969**, 31 (5), 1263–1282.

(30) Sueki, K.; Akiyama, K.; Kikuchi, K.; Nakahara, H.; Tomura, K. *J. Radioanal. Nuclear Chem.* **1999**, 239 (1), 179–185.

(31) Wahl, A. C.; Bonner, N. A. *Radioactivity Applied to Chemistry*; Wiley and Sons: New York, 1951; pp 511–515.

(32) *Handbook of Health Physics and Radiological Health*, 3rd ed., section 8–9; Shleien, B., Slaback, L. A., Jr., Birky, B. K., Eds.: Lippincott Williams & Wilkins: Baltimore, MD, 1998.

NOESY, and 2D-HSQC–TOCSY spectra. Carbon chemical shifts were identified through the HSQC and HMBC. Similarly, the chemical shifts of Lu-AMBA and Hf-AMBA were also identified (Tables 1S–3S, Supporting Information).

**The Structure of the Free Ligand.** In order to determine the solution structure of the free ligand, <sup>HN–HA</sup>*J* coupling constants were measured and the chemical shift index method<sup>33</sup> was performed. Both measurements indicated that the peptide is largely unstructured. The majority of the measured *J* couplings (Table S7, Supporting Information) are between 6 and 8 Hz, the range known to be most likely the result of conformational averaging. The chemical shift index (applied to the fragment QWAVGHLM) using H $\alpha$ , C $\alpha$ , C $\beta$ , and C' chemical shifts predicted coil conformation both in the free and in the complexed ligand (data not shown). Deviations from random coil values are limited, as reported in Figure 1S (Supporting Information).

Despite the evidence of consistent motion, we decided to determine at least an average structure by converting NOE intensities into distances. This is possible given the inverse relationship between the NOE and the distance:

$$\frac{r_{ij}}{r_{\text{ref}}} = \sqrt[6]{\frac{V_{\text{ref}}}{V_{ij}}}$$

where *V* and *r* are the intensity of the cross peak and the distance between protons *i* and *j*, respectively, and the subscript ref indicates these values for a pair of protons at a fixed distance. We used the cross peak between the geminal protons of DO3A (the ones adjacent to Gly) whose interproton distance was fixed at 0.175 nm. Using this reference, all other distance constraints (about 100) were evaluated (Tables S4–S6, Supporting Information) and used for structure calculation using torsional angle dynamics by the DYANA program.<sup>34</sup> The conformation of the monosubstituted DO3A chelator was minimized by HYPERCHEM (release 8.0 for Window, Hypercube Inc., 2007) and inserted into the DYANA library manually. As this is intended to be an average of multiple conformers, we allowed the constraints to vary by  $\pm 0.05$  nm.

Interestingly, a stacking interaction between the phenyl moiety of the linker and the side chain of tryptophan was clearly demonstrated by NOEs (Figure 4S, Supporting Information). Figure 7 shows the ensemble of the first best 30 structures obtained. By fitting the position of all backbone atoms, an ill-defined structure is obtained. The disorder reflects the high degree of motion present in the molecule. However, if we focus on the region between the aminobenzoyl moiety and the alanine (by fitting the position of these atoms), a well-defined motif is found (A panel) due to the stacking between the aromatic rings of the linker and the tryptophan residue of the peptide (B panel). This demonstrates a local order in the linker region for the AMBA ligand. This finding is intriguing, as we have previously found that <sup>177</sup>Lu-containing radiotherapeutic bombesin derivatives have

improved tumor uptake and retention properties when the linker between the DO3A–monoamide chelator and the targeting BBN<sup>7–14</sup>–NH<sub>2</sub> group contains a non- $\alpha$  amino acid bearing a cyclic aromatic group.<sup>35</sup>

**The Structure of the Lu and Hf Complexes.** The comparison of the chemical shifts of both complexes with those of the free ligand (Figure 2S, Supporting Information) clearly shows that most significant deviations are located on the DO3A moiety, due to the effect of metal coordination. The absence of shifts in the peptidic part demonstrates that the metal does not perturb this region of the structure. However, some nuclei in the linker between the peptide and the DO3A experience significant shifts in both complexes. The data indicate that the carbonyl between the Gly adjacent to DO3A and aminobenzoyl moieties could well be involved in the coordination (Figure 6). The disappearance of the cross peak between their amide protons and the doubling of the amide proton of Gln residue also demonstrate that the metal is perturbing this region (data not shown). Coordination of an amide carbonyl in a monosubstituted DO3A–monoamide-containing peptide has previously been described by Deshmukh et al.<sup>36</sup> for Y<sup>III</sup>–DOTATOC and observed by X-ray crystal structure in the Y<sup>III</sup>–DOTA–D–Phe–NH<sub>2</sub>.<sup>37</sup>

As we are in slow exchange conditions on the NMR time scale, NOE intensities can still be interpreted as interproton distances. For this reason, the procedure used for the free ligand was repeated, but the binding of the carbonyl belonging to the Gly residue of the linker and those of DO3A were included as a constraint in the structure calculation. Binding to the carboxylates and the amine nitrogens in DO3A was also imposed as a constraint. The results are shown in Figure 5S (Supporting Information).

The stacking found in the free ligand is also present in the complexes, although in the Hf complex this stacking seems less pronounced, most likely due to the poor quality of its NOESY spectra (because of partial precipitation of the sample). We believe that the stacking interaction is maintained, as a different conformation would result in different chemical shifts for the tryptophan and phenyl residues, and this was not observed. Some differences in the shifts of the Lu and Hf complexes were observed in the DO3A portion of the molecule and in the linker. Those differences have to be attributed to the different magnetic anisotropy tensors of the two metals rather than a substantial difference in coordination.

As no distance constraints could be derived for the region within the DO3A (due to severe overlap), we used a minimized structure of DO3A as a “frozen” conformation in the DYANA calculation. This frozen conformation did not allow the flexibility and rearrangements needed to harbor the new carbonyl ligands from the linker found experimentally. For this reason, we performed a minimization of the

(33) Wishart, D. S.; Sykes, B. D. *J. Biomol. NMR* **1994**, *4*, 171–180.

(34) Güntert, P.; Mumenthaler, C.; Wüthrich, K. *J. Mol. Biol.* **1997**, *273*, 283–298.

(35) Cappelletti, E.; Lattuada, L.; Linder, K. E.; Marinelli, E.; Nanjappan, P.; Raju, N.; Swenson, R. E. Improved gastrin releasing peptide compounds. WO 2005/067983, filed July 12, 2004.

(36) Deshmukh, M. V.; Voll, G.; Kühlewein, A.; Mäcke, H.; Schmitt, J.; Kessler, H.; Gemmecker, G. *J. Med. Chem.* **2005**, *48* (5), 1506–1514.

(37) Heppeler, A.; Froidevaux, S.; Mäcke, H. R.; Jermann, E.; Béhé, M.; Powell, P.; Hennig, M. *Chem.–Eur. J.* **1999**, *5*, 1974–1981.

complexes imposing only the coordination of the ligands to a generic metal, using a molecular mechanics OPLS force field available in the program HYPERCHEM. The results are shown in Figure 8. As shown in the figure, the geometry of the coordination sphere seems to easily accommodate the expected coordination of the DO3A carbonyls and the proposed coordination of the Gly carbonyl. Furthermore, without giving any kind of interproton structural restraints, the minimization reproduces the stacking experimentally observed.

From a practical point of view, the results described in this manuscript raise some potential questions. What is the actual amount of Hf that could be formed *in vivo*; does that amount pose any health risk; should these factors be underlying concerns for the use of Lu-177 radiopharmaceuticals?

We believe that the toxicological concerns are minimal. There are two kinds of Hf that must be considered: free  $^{177}\text{Hf}$  formed from the decay of  $^{177}\text{LuCl}_3$  prior to radiolabeling and  $^{177}\text{Hf}$ -containing products formed from the decay of their  $^{177}\text{Lu}$ -labeled parents.

On the basis of a typical  $^{177}\text{Lu}$  specific activity at the end of a target irradiation (EOB) of 25 Ci/mg, a 200 mCi sample of  $^{177}\text{Lu}$  at EOB will contain an estimated  $\sim 0.5 \mu\text{g}$  of Hf formed from the decay of  $^{177}\text{Lu}$  during irradiation. This “free” Hf is most likely to be in the form of polymeric Hf species, as was reported for the structure of  $\text{HfOCl}_2 \cdot \text{XH}_2\text{O}$  in HCl.<sup>19</sup> The amount of Hf in the radioisotope will increase as the  $^{177}\text{Lu}$  stock solution decays but is unlikely to exceed 1  $\mu\text{g}$  of Hf/200 mCi dose. As shown in our work, and that of Breeman et al.,<sup>12</sup> such free Hf does not react with DO3A—monoamide chelators, so it will be present in all unpurified radiotherapy doses of  $^{177}\text{Lu}$ . Such amounts ( $\sim 1 \mu\text{g}/70 \text{ kg}$ ) of “free” Hf have been injected into hundreds of patients during radiotherapy with the somatostatin receptor binding compound [(177Lu)-DOTA(0), Tyr(3)]octreotate, which is under evaluation for the radiotherapeutic treatment of neuroendocrine tumors.<sup>38</sup> In these studies, relatively few adverse effects were observed, and these are most likely due to the high doses of  $^{177}\text{Lu}$  used for treatment. Such effects are readily justified due to the undeniable benefits of treating the underlying cancer.

The other form of Hf that must be considered is that which forms through the decay of  $^{177}\text{Lu}$ -bearing radiopharmaceuticals. For  $^{177}\text{Lu}$ -AMBA that decays to  $^{177}\text{Hf}$ -AMBA, the metabolic fate of the decay product is likely similar to that of the parent compound. We have found that  $^{177}\text{Lu}$ , following IV injection of  $^{177}\text{Lu}$ -AMBA in tumor-bearing mice, is almost completely cleared from most normal tissue within 24 h of injection<sup>4</sup> but clears slowly from tissue bearing the GRP receptor-bearing tissues to which this compound is targeted. We theorize that the corresponding Hf-AMBA complex (and metabolites) would be cleared faster than those of Lu-AMBA

due to its increased charge. The metabolic fate of any nonradioactive Hf that is lost from the chelator is likely to be similar to that described by Ando and Ando,<sup>39</sup> who studied the biodistribution of  $^{181}\text{Hf(IV)}$  chloride in tumor-bearing rats.  $^{181}\text{Hf}$  was found to localize in the liver, spleen, and bone, consistent with a colloidal or polymeric composition. The toxicology literature indicates that the injection of microgram levels of Hf is not of toxicological concern. Studies in cats showed no toxicity upon 0.5–2 mg/kg IV injection of  $\text{HfOCl}_2 \cdot 8\text{H}_2\text{O}$ , and the intraperitoneal LD<sub>50</sub> following 7 days of treatment with  $\text{HfOCl}_2$  in rats was 112 mg/kg.<sup>40</sup>

## Conclusion

In this study, we provide the first report of a Hf-DO3A-containing compound and demonstrate that  $^{177}\text{Hf}$ , when formed by the decay of  $^{177}\text{Lu}$ -AMBA, is retained in the monosubstituted DO3A chelator and results in stable  $^{177}\text{Hf}$ -AMBA complexes. Hf-AMBA, which exists as a pair of isomers, has been synthesized and fully characterized by EA, NMR, MS, and HPLC coinjection studies, though the precise nature of the isomeric difference has not been established. NMR data also show structural similarities between Hf-AMBA and the Lu-AMBA compound and support the assumption that hafnium is retained by AMBA in the oxidation state IV. The identity of the radiotherapeutic complex  $^{177}\text{Lu}$ -AMBA has been confirmed by coinjection studies with a fully characterized sample of  $^{177}\text{Lu}$ -AMBA.

**Acknowledgment.** The authors thank Prof. Michael J. Welch and Dr. William C. Eckelman for their insights into the literature of isolated products of  $\beta$  decay. Discussions with Dr. Michael H. Brill regarding methods for the calculation of recoil energy are also gratefully acknowledged. We thank Bruker Biospin srl for providing a 600 MHz spectrometer (Bruker Avance III Ultra Shield Plus) and CBM (Consorzio per il Centro di Biomedicina Molecolare S.c.r.l., AREA Science Park, Basovizza, Trieste, Italy) for hosting the instrumentation.

**Supporting Information Available:**  $^1\text{H}$  and  $^{13}\text{C}$  assignments for AMBA ligand (Table S1), Lu-AMBA (Table S2), and Hf-AMBA (Table S3). Experimental distance constraints from NOESY cross-peaks for free AMBA (Table S4), Lu-AMBA (Table S5), and Hf-AMBA (Table S6). Figure 1S: Chemical shift deviations from random coil values for AMBA ligand. Figures 2S and 3S: Proton and carbon chemical shift deviations of Lu-AMBA and Hf-AMBA complexes with respect to the AMBA ligand and each other. Figure 4S: Long-range NOEs in AMBA. Figure 5S: Selected structures of Lu-AMBA and Hf-AMBA complexes. This material is available free of charge via the Internet at <http://pubs.acs.org>.

IC802328A

(38) Kwekkeboom, D. J.; de Herder, W. W.; Kam, B. L.; van Eijck, C. H.; van Essen, M.; Kooij, P. P.; Feelders, R. A.; van Aken, M. O.; Krenning, E. P. *J. Clin. Oncol.* **2008**, *26* (13), 2124–2130.

(39) Ando, A.; Ando, I. *Int. J. Radiat. Appl. Instrum. B* **1986**, *13* (1), 21–29.

(40) Haley, T. J.; Raymond, K.; Komesu, N.; Upham, H. C. *Toxicol. Appl. Pharmacol.* **1962**, *4*, 238–246.